SANDIA REPORT
SAND97-1172 • UC-701
Unlimited Release
Printed May 1997

LDRD Final Report on Chemical Functionalization of Oligo(hydrido)silanes, Economically Attractive Routes to New Photoresponsive Materials

Gregory M. Jamison, Douglas A. Loy, Celeste N. Rohlfing, John G. Curro,
Glen Kepler, Kimberly A. Opperman

Prepared by
Sandia National Laboratories
Albuquerque, New Mexico 87185 and Livermore, California 94550

Sandia is a multiprogram laboratory operated by Sandia Corporation, a Lockheed Martin Company, for the United States Department of Energy under Contract DE-AC04-94AL85000.

SF2900Q(8-81)

Issued by Sandia National Laboratories, operated for the United States Department of Energy by Sandia Corporation.

Available to DOE and DOE contractors from
Office of Scientific and Technical Information
P.O. Box 62
Oak Ridge, TN 37831

Prices available from (615) 576-8401, FTS 626-8401

Available to the public from
National Technical Information Service
U.S. Department of Commerce
5285 Port Royal Rd
Springfield, VA 22161

NTIS price codes
Printed copy: A03
Microfiche copy: A01

SAND 97-1172
Unlimited Release
Printed May 1997

Distribution
Category UC-701

LDRD Final Report on Chemical Functionalization of Oligo(hydrido)silanes, Economically Attractive Routes to New Photoresponsive Materials

Gregory M. Jamison, Douglas A. Loy, Celeste M. Rohlfing, John G. Curro, Glen Kepler and Kimberly A. Opperman
Electronic and Optical Materials Department
Sandia National Laboratories
P.O. Box 5800
Albuquerque, NM 87185-1405

Abstract

Metathesis-catalyzed polymerizations of primary silanes were performed to generate polysilanes suitable for functionalization with a variety of side groups. Modeling was employed to predict conformations and estimate electronic properties of candidate functionalized polysilanes. Chemical functionalization of oligo(hydrido)silanes with terminal α,ω-dienes under free radical conditions yielded highly crosslinked, nonporous polysilane networks. Ketone reduction with oligo(hydrido)silanes under free radical conditions led to novel poly(phenylalkoxysilanes). Free radical reduction of terminal alkenyl(alkoxy)silanes forms functionalized polysilanes which can be further transformed into sol-gel matrices with the polysilane functionality intact. These gels may be processed into nonporous xerogels or high surface area aerogels.

CONTENTS

DISCLAIMER

LDRD Final Report on Chemical Functionalization of Oligo(hydrido)-silanes, Economically Attractive Routes to New Photoresponsive Materials

Introduction

This project was designed to develop new, environmentally friendly routes to novel polysilanes as possible alternatives to organic photoconductors for electrophotographic applications, sensor materials and LED devices.

Polysilanes have been the subject of fundamental and applied research due to their electronic properties, which are similar to polyconjugated organic materials, despite the fact that polysilanes have a fully saturated, linear molecular structure. Delocalization of σ-bonding electrons into energetically accessible σ* antibonding orbitals is cited for the unusually long wavelength, low energy transitions. This electronic excitation can be stimulated by low intensity UV light (some polysilanes can absorb in the visible region of the spectrum) and are sensitive to conformation and substitution along the all-silicon backbone. Many polysilanes are photosensitive and undergo backbone cleavage, a trait which makes them useful as self-developing photoresists. Additionally, poly(phenylmethyl)silane has been shown to be a good photoconductor, with hole mobilities measured up to 10^{-4} $cmV^{-1}sec^{-1}$ upon low intensity laser excitation at electric fields on the order of 10^5 Vcm^{-1}. Quantum efficiency for this system is approximately 1%. Both quantum efficiency and hole mobility for poly(phenylmethyl)silane exceed the performance of organic photoconductors used in electrophotographic applications.

Despite the promise polysilanes hold as superior photoconductors for the electroimaging industry, their widespread employment has not been realized to date. This is due, in part, to the safety and environmental considerations involved in preparing high molecular weight polysilanes on an industrial scale. The traditional synthetic approach to forming polysilanes involves the reduction of hydrolytically sensitive dichlorosilanes with pyrophoric alkali metals or suitable alloys such as Na/K. The reductions take place at reflux temperatures of high-boiling organic solvents at high dilution, leading to appreciable amounts of organic waste. Control of the product's molecular weight and substitution pattern are minimal, as bimodal molecular weight distributions are almost always realized, and only the most robust organic side groups are able to survive under these Würtz coupling conditions.

Through catalytic σ-bond metathesis polymerization of primary silanes under mild conditions we have accessed a variety of novel polysilane materials via post-polymerization

functionalization of the polysilane backbone. Our approach has involved 1. The *ab initio* molecular modeling of isolated linear oligosilane molecules to establish equilibrium geometries associated with various backbone conformations and polarizabilities for macromolecular polysilanes, 2. Monte Carlo simulations to gain insight into polysilane chain conformation preferences (electronic localization as a coil vs. electronic polyconjugation in extended conformations) and 3. free radical hydrosilation of unsaturated reagents for derivatization of oligo(hydrido)silanes and manipulation of the functionalized materials into gels whose bulk properties can be controlled by choice of processing.

We have established a methodology for generating robust, crosslinked materials as potential precursors to silicon carbide and photochromic glasses. The sol-gel polymerization of alkoxysilane-substituted polysilanes has led to the formation of the first polysilane/polysiloxane nanocomposite materials with controllable porosity and surface area characteristics.

Results

Results from this project were informative as to the possibility of preparing robust crosslinked materials containing the polysilane chromophore. The participants on this project have made significant contributions to understanding the conformational dependence of the low energy σ-σ^* transitions in model oligosilanes, the statistical estimation of their conformation in the bulk phase, the preparation of primary oligo(hydrido)silanes $[(H)(Ph)Si]_n$, and their manipulation into robust hybrid materials. The remainder of the report is a summary, including a list of publications and presentations, describing the research areas impacted by this LDRD: "*Ab Initio* Molecular Modeling of Oligophenylsilanes," "Statistical Analysis of Polysilane Chains" and "Chemical Functionalization of Oligophenylsilane."

1. *Ab Initio* Molecular Modeling of Oligophenylsilanes

Computer modeling studies were conducted by *ab initio* calculations of a number of oligophenylsilanes. More detailed electron correlated *ab initio* calculations (3-21G*) have established equilibrium geometries associated with various linear conformations to better approximate rotational barriers and to parameterize these systems for molecular mechanics modeling. We were able to conclude that a standard set of geometrical parameters should be acceptable for studies of longer oligomers and high polymers. Furthermore, oligomer

polarizabilities were calculated and utilized for statistical mechanical calculations. The HF/3-21G* level calculations are acceptably accurate. Polarizability determination for helical conformations should be investigated.

Structures

Geometry optimizations performed at the HF/3-21G* level on $Si_3(C_6H_5)_3H_5$ and $Si_4(C_6H_5)_4H_6$ showed no significant variation in bond lengths or bond angles between the two molecules. The phenyl rings are placed in parallel planes to begin the optimizations. Below is a summary of optimized bond lengths and angles.

Parameter	$Si_3(C_6H_5)_3H_5$	$Si_4(C_6H_5)_4H_6$
Si--Si	2.348--2.353	2.350--2.354
Si--C	1.879--1.887	1.878--1.887
Si--H	1.479--1.482	1.479--1.483
C--C	1.382--1.397	1.383--1.397
C--H	1.072--1.074	1.072--1.074
Si--Si--Si	111.3	111.7
Si--Si--H	108.7--110.1	108.6--109.2
Si--Si--C	110.7--112.3	109.3--112.6
C--C--C	119.8--121.1	119.8--121.1
C--C--H	118.9--121.1	118.8--121.2

These results suggest that a standard set of geometrical parameters may be adopted in studies of longer oligomers.

Complete geometry optimizations at the MP2/6-31G* level were carried out for $Si_3(C_6H_5)_2H_6$. These results were used to estimate a set of assumed parameters for use in calculations on longer oligomers. Lengthy geometry optimizations at the same level were undertaken subsequently for $Si_3(C_6H_5)_3H_5$. Results of this calculation are compared to the assumed parameters estimated from the $Si_3(C_6H_5)_2H_6$ calculation in the table below. The full optimization confirms the accuracy of the assumed parameters, which are used in all calculations henceforth.

Parameter	Assumed	Optimized
Si--Si	2.343	2.345 Å
Si--C	1.882	1.882--1.886
Si--H	1.492	1.492--1.496
C--C	1.400	1.397--1.409
C--H	1.095	1.088--1.090
Si--Si--Si	107	108°
Si--Si--H	110	109
Si--Si--C	109	112
C--C--C	120	118--121
C--C--H	120	119--121

Rotation Barriers

Rotation barriers were calculated at the HF/3-21G* level for $Si_4(C_6H_5)_4H_6$ starting from the $\Theta = 60°$, all--anti structure (Θ is the dihedral angle between consecutive Si--C bonds; in the all-anti structure of $Si_4(C_6H_5)_4H_6$, all Si--C bonds lie above the plane of the four Si nuclei). When the Si--Si--Si--Si dihedral angle is rotated from 180° to -60°, the total energy declines by 17 kcal/mole. Positive rotations lead to a rapidly ascending total energy produced by a close approach between two phenyl rings on Si_1 and Si_3. (Reoptimizations of dihedral angles of the rings relative to the Si backbone were not attempted).

Si--Si--Si--Si	E_{total} (a.u.)	ΔE (kcal/mole)
-180	-2079.61254	16.6
-170	-2079.62268	9.8
-160	-2079.62836	6.3
-150	-2079.63207	3.9
-140	-2079.63456	2.4
-130	-2079.63591	1.5
-120	-2079.63639	1.2
-110	-2079.63647	1.2
-100	-2079.63662	1.1
-90	-2079.63704	0.8
-80	-2079.63762	0.5
-70	-2079.63814	0.1
-60	-2079.63835	0.0

(cont'd.)

Si--Si--Si--Si	E_{total} (a.u.)	ΔE (kcal/mole)
-50	-2079.63796	0.2
-40	-2079.63605	1.4
-30	-2079.62999	5.2
-20	-2079.61668	13.6
-10	-2079.59484	27.3
0	-2079.50742	82.2

Polarizabilities

Comparisons of HF/3-21G* and HF/6-31G* polarizabilities were performed at the standard geometries of the $\Theta = 60°$ isomers of $Si_4(C_6H_5)_4H_6$ and $Si_5(C_6H_5)_5H_7$. In the same set of arbitrary coordinates, the results are as follows for the $\Theta = 60°$ case.

Polarizabilities

	a_{xx}	a_{xy}	a_{yy}	a_{xz}	a_{yz}	a_{zz}
$Si_4(C_6H_5)_4H_6$ 3-21G*	233.730	86.565	313.748	0.0	0.0	313.402
$Si_4(C_6H_5)_4H_6$ 6-31G*	259.865	82.153	328.316	0.0	0.0	324.593
$Si_5(C_6H_5)_5H_7$ 3-21G*	240.390	5.701	448.472	0.775	1.132	379.189
$Si_5(C_6H_5)_5H_7$ 6-31G*	275.888	5.236	464.380	0.722	1.315	392.331

The 3-21G* and 6-31G* calculations are in reasonable agreement: the traces of the polarizabilities are within 6% of each other. Because the 6-31G* calculations take approximately four times as much cpu time to execute, the 3-21G* basis is an advantageous compromise of accuracy and efficiency.

Results on polarizabilities are presented henceforth in a standard reference frame. Coordinates were chosen such that z is the polymer translation axis and x is the perpendicular axis lying in the plane defined by the Si nuclei. Two kinds of all-anti chains are considered: $\Theta = 60°$ and $\Theta = 180°$.

Polarizabilities for larger chains, where the number of unit cells, N, is large are calculated by fitting results for four chains to a series,

$$\frac{\alpha(N)}{N} = a_1 + \frac{a_2}{N} + \frac{a_3}{N} + \frac{a_4}{N}$$

Polarizabilities for $\Theta = 60°$

N	a_{zz}	a_{xx}	a_{yy}	a_{xy}	a_{xz}	a_{yz}
4	174.124	348.844	353.324	72.282	-14.961	-10.159
5	231.669	425.943	431.337	90.688	-1.103	-.764
6	292.291	502.815	508.884	109.190	14.142	9.783
7	355.190	578.569	585.427	127.055	-1.079	-.741
8	419.623	654.203	661.750	144.953	-16.925	-11.780
$N \rightarrow \infty$ (4--7)	71.0N	68.3N	70.6N			
8 (estim.)	419.739	653.192	661.020			
$N \rightarrow \infty$ (5--8)	69.8N	79.1N	78.4N			

Polarizabilities for $\Theta = 180°$

N	a_{zz}	a_{xx}	a_{yy}	a_{xy}	a_{xz}	a_{yz}
4	180.192	367.286	313.402	.000	-18.527	.000
5	240.237	448.257	379.557	5.155	-1.032	-.591
6	303.542	528.966	444.953	.000	17.976	.000
7	369.264	608.436	509.814	-4.899	-.979	-.572
8	436.634	687.812	574.364	.000	-20.642	.000
$N \rightarrow \infty$ (4--7)	74.4N	71.3N	63.1N			
8 (estim.)	436.739	686.655	574.296			
$N \rightarrow \infty$ (5--8)	73.2N	83.6N	63.8N			

The asymptotic polarizabilities per unit cell are given by a_1. When this procedure employs results for $Si_4(C_6H_5)_4H_6$ through $Si_7(C_6H_5)_7H_9$ to obtain the *a* coefficients, the resulting equation is used to predict polarizabilities for $Si_8(C_6H_5)_8H_{18}$. These predictions are in close agreement with the calculated values for the latter oligomer. The procedure is repeated using results from $Si_5(C_6H_5)_5H_7$ through $Si_8(C_6H_5)_8H_{10}$. The two predictions for the large N limit also are in close agreement.

2. Statistical Analysis of Polysilane Chains

Monte Carlo statistical mechanics were conducted for polysilane solutions from the detailed *ab initio* calculations. Others have demonstrated that coil/rod transitions occur in polysilane solutions as the temperature is lowered below a critical value. This prediction is

consistent with UV spectroscopic studies. However, others have questioned this prediction. In order to qualitatively study polysilanes in solution we have employed a model of a rotational isomeric state chain. The chain segments interact via a hard core repulsion with superimposed attractive interactions of the Lennard-Jones type. Such a model represents an "ordinary chain" in solution. A second model was also studied which represents a polysilane macromolecule. The polysilane chain is like the ordinary chain, except that those repeat units that are part of a trans sequence of rotational states along the chain backbone have an extra polarizability due to electronic delocalization facilitated by trans bonds. This polarizabilty increment caused, by sigma conjugation, would be expected to depend on the number of bonds making up the run of consecutive trans states. This model subjects the polysilane chain to a "frustration" effect. On one hand the chain will want to collapse as the solution is cooled due to enhanced polymer/polymer attractions. On the other hand the chain can increase its polymer/polymer attractive interactions by expanding to form long sequences of trans states along the chain backbone.

We studied the above polysilane frustration model using Monte Carlo simulation techniques for chains of N=50 repeat units. For purposes of illustration it was assumed that the polarizability increment scales quadratically with the number of consecutive trans states with a cutoff at 10 bonds. The average size of the chain, as measured by the characteristic ratio defined as $C_n=\langle r^2\rangle / NL^2$, where $\langle r^2\rangle$ is the mean square end-to-end distance of the chain and L is the bond length, was followed as a function of temperature. Fig. (1) shows results for both the "ordinary chain" and a polysilane chain. Note that in both types of chains the average size decreases as the temperature is lowered in a manner consistent with the intrinsic viscosity experiments. To characterize the extent of delocalization along the chain backbone we define a delocalization length $\xi = \langle N_{max}\rangle/N$, where $\langle N_{max}\rangle$ is the maximum run of trans states on an average chain. Fig. (2) depicts ξ as a function of temperature. Note that the delocalization length of the polysilane chain increases, in contrast to the ordinary chain, in a manner which is consistent with the observed red shift in the UV measurements of Harrah and Zeigler.

These Monte Carlo simulations have demonstrated that the electron delocalization model, originally proposed by Schweizer, is consistent with both UV spectroscopy and intrinsic viscosity experiments. Rather than undergoing a coil/rod transition as proposed by Schweizer, we have demonstrated that the polysilane chains tend to form collapsed structures in solution. These collapsed chains have long runs of trans states along their backbone, but can fold back on themselves due to the presence of occasional gauche defects.

Fig. 1: Characteristic Ratio from
Monte Carlo Simulation, N=50

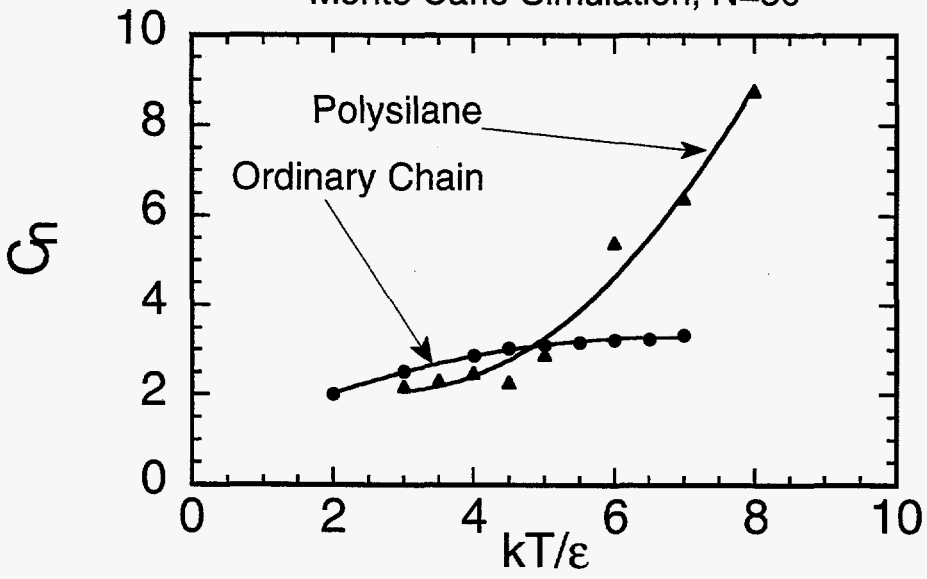

Fig. 2: Electron Delocalization Length
from Monte Carlo Simulation, N=50

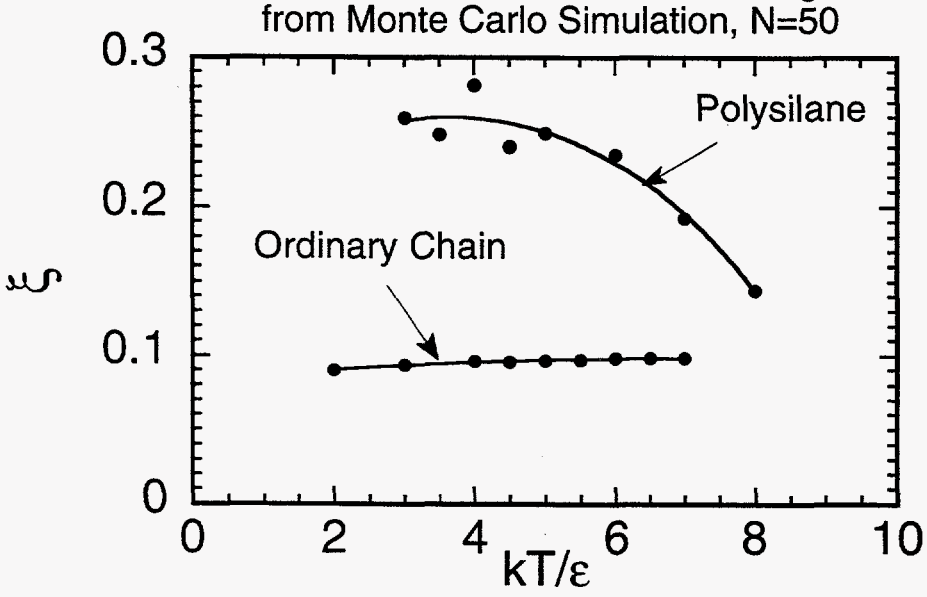

3. Chemical Functionalization of Oligophenylsilane

Zirconocene-catalyzed Si-H σ-bond metathesis of phenylsilane generates oligophenylsilane (Scheme 1). This approach is a safe, economically attractive alternative to reductive coupling of dichlorosilanes. Additionally, there is greater latitude in the ability to chemically functionalize oligophenylsilane by taking advantage of the Si-H bond in the $[(H)(Ph)Si]_n$ repeat unit.

Scheme 1

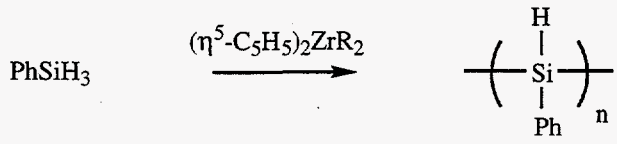

We have conducted free-radical initated hydrosilation of aldehydes and ketones and successfully formed new alkoxy-substituted polysilane derivatives (**A**, eq. 1). For example, reduction of acetone results in poly(isopropoxy)(phenyl)silane; salient characteristics include a red shift in the UV spectrum from approx. 300 nm to 340 nm. A potential application for the polysilane sol-gels may be as light exposure indicators (use control agents). We have performed photobleaching of neat polysilanes *and polysilane sol-gels* under high intensity light, resulting in the loss of their characteristic high wavelength UV absorption (Fig. 3) and will continue to develop them as potential UV-sensitive coatings.

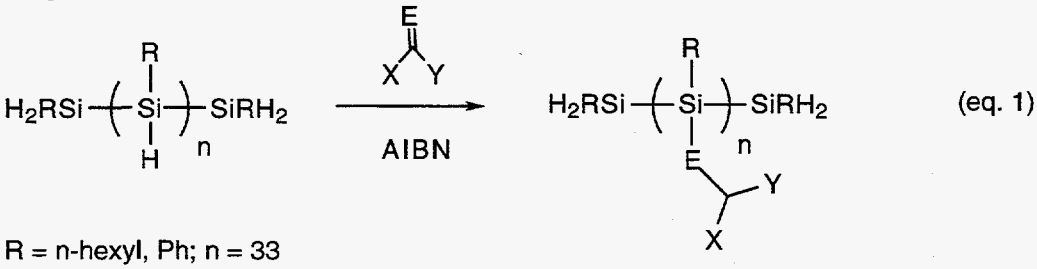

(eq. 1)

R = n-hexyl, Ph; n = 33

E = O, X = Y = Me (**A**)

E = $CH(CH_2)_2CH{=}CH_2$, X = Y = H; organic crosslinking matrix (**B**)

E = CH_2, X = H, Y = $Si(OEt)_3$; siloxane crosslinking matrix (**C**)

Novel Hybrid Polysilane Networks: The ability to entrain photoconducting materials into stable organic or siloxane matrices may prove beneficial to commercial applications (xerography, LED displays) where harsh service conditions (high temperature, oxidative environment) demand thermally robust, stable photoconductors.

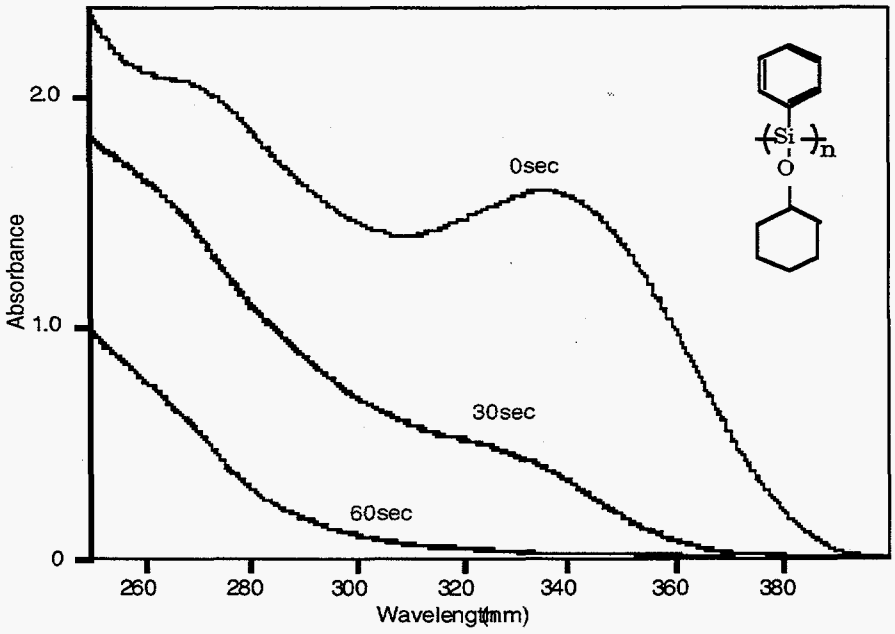

Figure 3. Photobleaching study of neat film of poly(cyclohexyloxy)(phenyl)silane.

We have made new polysilane graft copolymers by employing aliphatic α,ω-dienes as organic crosslinking agents (**B**) to join separate polysilane chains in a one-step free radical-initiated hydrosilation reaction; these materials have been characterized as thermally robust, nonporous glasses (T_C ~ 430° C, N_2 atmosphere). Time-of-flight photoconductivity measurements have been performed and show low but erratic photocurrents. Comparative studies of crosslinker substitution (branching) and structure (rigid vs. flexible) effects on porosity, thermal stability and ceramic yield and photocurrent are in progress.

We have applied this approach to include (alkoxysilyl)propyl functionalities as latent sol-gel polymerizable residues for the preparation of a new class of hybrid organic-inorganic polysilane-siloxane materials, derived from the sol-gel polymerization of functionalized polysilanes **2a-c** (eq. 2). Free radical-initiated hydrosilation of allyl(ethoxy)silanes **1a-c** with polyphenylsilane leads to efficient backbone elaboration with little degradation of the silicon catenate (eq. 2). GPC analysis of functionalized poly(triethoxysilylpropyl)(phenyl)silane **2a** indicates that a small amount of degradation, probably to form stable cyclic oligomers, has taken place, but that the majority of material

remains as linear polymer of modest molecular weight (for **2a**, M_w = 10,635; M_w/M_n = 1.23).

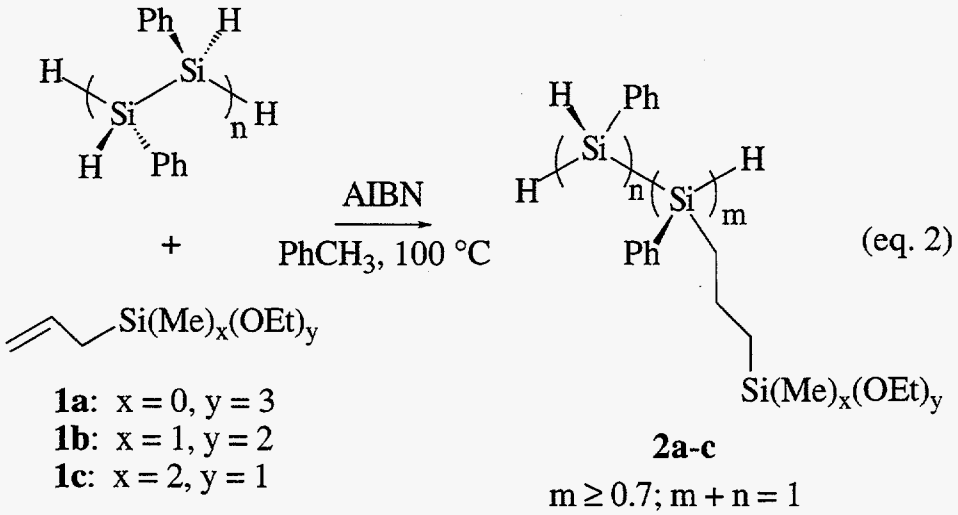

(eq. 2)

1a: x = 0, y = 3
1b: x = 1, y = 2
1c: x = 2, y = 1

2a-c

$m \geq 0.7$; $m + n = 1$

Integration of the ^1H NMR spectrum of functionalized polysilanes **2a-c** yields information regarding the degree of polysilane backbone substitution; in all cases hydrosilation of allyl silanes **1a-c** yielded polysilanes with 70% or greater substitution. This is corroborated by inspection of the infrared spectra (comparison of the intensity of the Si-H stretching band relative to the aromatic fingerprint region) to give a semi-quantitative value for the amount of backbone silicon substitution. The sol-gel precursors have also been characterized by solution ^{13}C and ^{29}Si NMR.

Hydrolysis-condensation of the ethoxysilane groups under acid-catalyzed conditions (5 mol% HCl, in ethanol) yields opaque white gels **3a-c** within 4 hours (eq. 3). (It is interesting to note that under basic conditions no gels form, and in fact polysilane backbone degradation takes place). The gels can be processed to give nonporous xerogels by washing with excess water and vacuum drying, or processed as aerogels by solvent extraction under a supercritical CO_2 atmosphere to give materials with modest surface areas; the dried samples were ground prior to analyses.

All dried gels were determined to be amorphous by x-ray diffraction analysis. Solid state ^{13}C NMR spectra (CPMAS NMR) of the xero- or aerogels confirm the retention of the aromatic and aliphatic (propyl) organic groups under the sol-gel reaction conditions. For example, the ^{13}C NMR of xerogel **3b** displays aromatic resonances at approximately 137 and 127 ppm; two aliphatic signals appear at 20 and 0 ppm, assigned to the propylene chain and the terminal methyl group of the siloxane D^n silicons (n = 1, 2, *vide infra*).

^{29}Si CPMAS NMR reflects two general types of silicon environment; polysilane backbone silicons generate a broad signal at -34 ppm in **3b**, and both partially condensed

D^1 and fully condensed D^2 siloxane silicons can be identified at -17 and -20 ppm, respectively (Fig. 4).

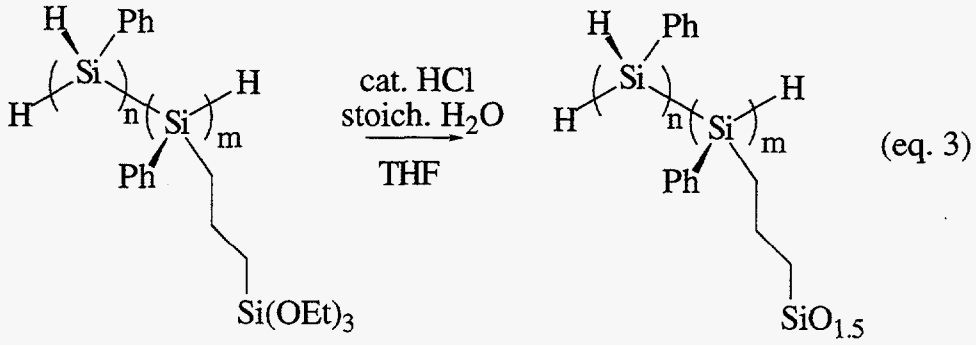

(eq. 3)

2a **3a**

When the solutions are cast as thin films, solid state UV-Vis spectroscopy confirms the retention of the polysilane backbone, reflected in the characteristic long wavelength absorption at $\lambda = 320$ nm for **3a** (Fig. 5). The polysilane-polysiloxane composites also display typical photobleaching behavior upon irradiation with UV light.

Nitrogen sorption analysis of the polysilane-polysiloxane nanocomposites indicate that the xerogels are nonporous. However, mesoporous aerogels of modest surface area (Type IV isotherm; ≈ 420 m^2/g for aerogel of **3a**; BET) result from supercritical CO_2 processing of the polysilane-polysiloxane wet gels. Scanning electron microscopy corroborates the aerogel mesoporosity, displaying granular fracture surfaces with particle diameters approximately 60 nm across.

SUMMARY

Theoretical advances have been realized in predicting the molecular structure and dynamics of oligosilanes which will be useful for understanding the relationships between polymer molecular structure and electronic behavior. Structural parameters for the modeling of $Si_n(C_6H_5)_nH_{(2n+2)}$ polymers have been obtained from accurate, *ab initio* calculations. Information on rotational barriers that will be of use to molecular modelers has been obtained as well. Polarizabilities per unit cell have been inferred from oligomer calculations for two kinds of all-anti polymers that differ in their C--Si--Si--C dihedral angles. The latter data are needed in statistical models of rod-coil phase transitions.

These studies should be extended in the following ways. Polarizabilities should be calculated for helical oligomers with several twist angles in order to infer unit cell polarizabilities. The dependence of the latter quantities on Si--Si--Si--Si dihedral angles

can be incorporated in model Hamiltonians. Statistical modeling that requires unit cell polarizabilities as a function of dihedral angles along the Si backbone will profit from this information.

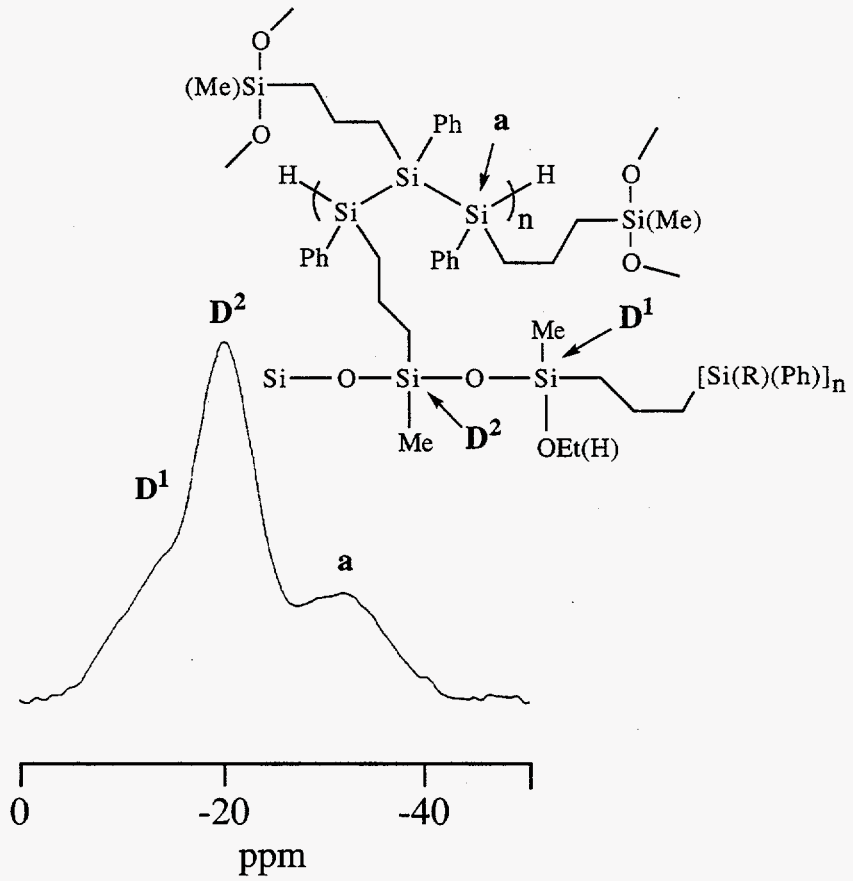

Figure 4. ^{29}Si CPMAS NMR spectrum of hybrid polysilane-polysiloxane xerogel **3b**.

AIBN-initiated functionalization of polyphenylsilane with allyl(ethoxy)silanes generates (ethoxysilylpropyl)polysilanes in good yield; this family of compounds serves as precursors for a new class of hybrid materials. Novel, amorphous polysilane-polysiloxane hybrid nanocomposites can be prepared by the mild, acid-catalyzed sol-gel hydrolysis-condensation of polysilane-based precursors **2a-c** at the pendant alkoxysilane residues. UV-Vis and multinuclear NMR spectroscopies establish the retention of the polysilane chromophore and attached organic residues; NMR also reflects the degree of condenstion at the siloxane silicon nuclei. The bulk morphology of the resulting dried gels can be

influenced by the choice of solvent removal from the wet gel. Aqueous extraction of solvent results in nonporous xerogels, while solvent removal by supercritical CO_2 yields mesoporous aerogels with retention of the wet gel surface area. The flexibility in manipulating the bulk morphology of these materials as it relates to electrochromic behavior still must be addressed.

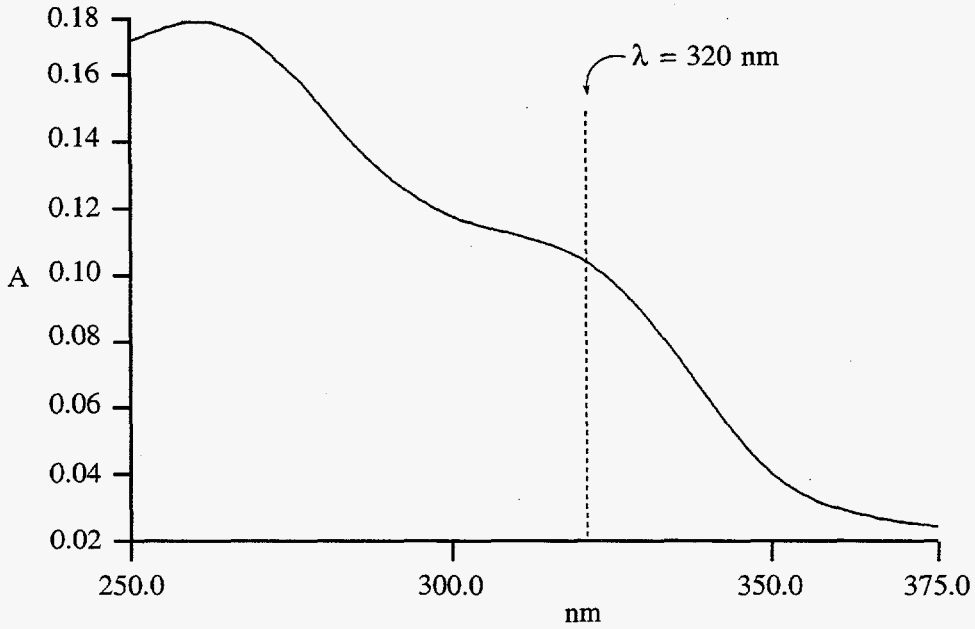

Figure 5. Solid state UV-Vis spectrum of polysilane-polysiloxane **3a**.

Time-of-flight photophysical measurements do not indicate formation of any long-lived charge-separated species. The possibility that these materials may be good *electron* conductors, as opposed to the hole-conducting characteristics of Würtz-coupled poly(methylphenylsilane) still must be addressed.

Presentations and Publications

1. *Hydrocarbon-Bridged Oligosilanes. A Novel Class Of Hybrid Crosslinked Organosilicon Materials*, K. A. Opperman, J. V. Beach, G. M. Jamison, D. A. Loy, and R. M. Waymouth. Presented as a poster at the 28th Organosilicon Synposium, Gainsville, FL, March 31-April 1, 1995.

Abstract

A new class of highly-crosslinked nonporous oligosilanes has been synthesized and investigated. Hexylene - (**1**) and 2, 5-dimethylhexylene - (**2**) bridged oligosilanes can be prepared by free-radical-initiated hydrosilation of 1, 5-hexadiene and 2, 5-dimethylhexadiene (respectively) with oligophenylsilane. The new materials' syntheses and characterization by IR, multinuclear solution (^{1}H, ^{13}C, and ^{29}Si) and solid state NMR, and UV-Vis spectroscopies, as well as nitrogen sorption porosimetry and thermal analysis, will be discussed.

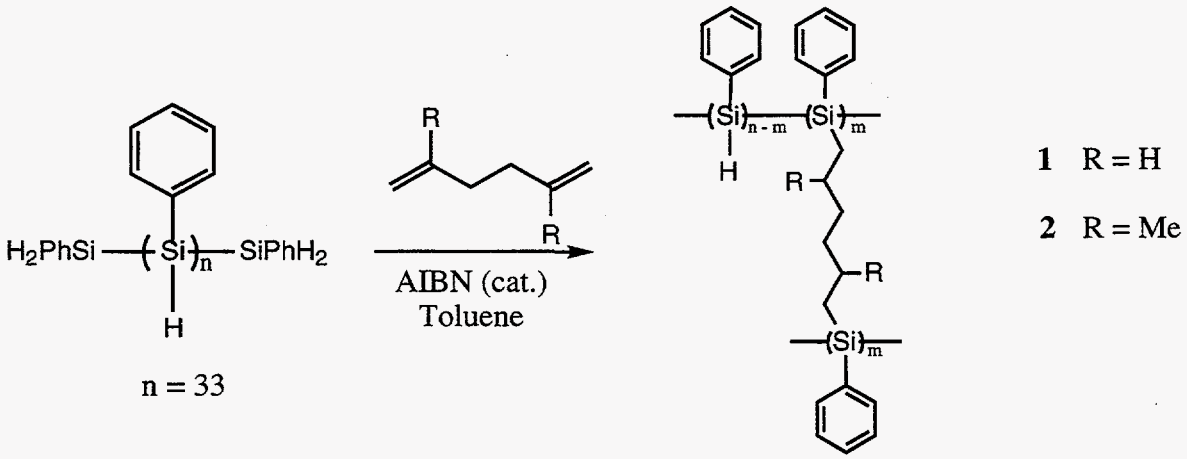

2. *Oligosilane-Siloxane Nanocomposites*, G. M. Jamison, D. A. Loy, K. A. Opperman, J. V. Beach and R. M. Waymouth. Presented at the 1996 Spring MRS Meeting, San Francisco, CA, April 8-12, 1996.

Abstract

Zirconocene-catalyzed σ-bond metathesis of phenylsilane is a mild and convenient way to generate synthetically versatile oligophenylsilane $[Si(H)(Ph)]_n$ ($n \approx 33$). Free radical-initiated hydrosilation of alkoxysilanes $RSiMe_x(OEt)_y$ (R = allyl; x = 0, y = 3; x = 1, y = 2; x = 2, y = 1) at the oligophenylsilane Si-H bonds, followed by sol-gel hydrolysis-polycondensation, yields novel siloxanes containing the intact oligosilane chromophore.

The sol-gel precursors and resulting siloxane materials have been characterized by solution and solid state multinuclear NMR, UV-VIS and IR spectroscopies and elemental analysis, and their bulk properties assessed by scanning electron microscopy, thermal and nitrogen sorption surface area analyses. The new materials' molecular and bulk properties, and the significance of processing and siloxane content on these properties, will be discussed.

3. *New Hybrid Polysilane-Polysiloxane Nanocomposites*, G. M. Jamison, D. A. Loy, K. A. Opperman, J. V. Beach and R. M. Waymouth. Presented as a poster at the 212th ACS National Meeting, Orlando, FL, August 25-29, 1996.

Abstract

(Alkoxysilyl)propyl-functionalized polysilanes 2a-c are generated by the free radical-initiated hydrosilation of allylsilanes 1a-c with polyphenylsilane. The latent sol-gel alkoxysilane residues undergo hydrolysis-polycondensation under acid-catalyzed conditions to form new hybrid organic-inorganic nanocomposites 3a-c, which can be processed as xerogels of aerogels. Spectral and bulk characterization of the new materials will be discussed.

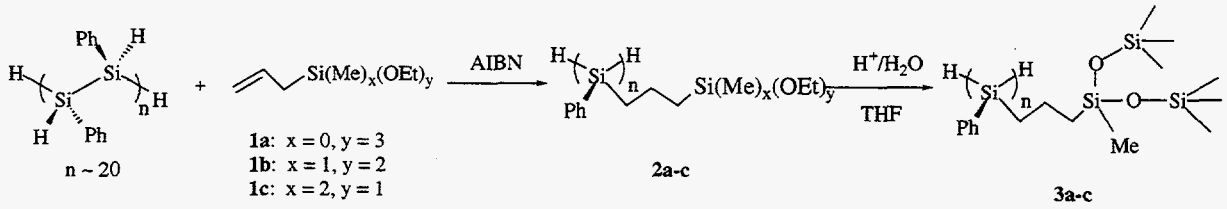

4. *New Hybrid Polysilane/Polysiloxane Nanocomposites.* Jamison, G. M.; Loy, D. A.; Opperman, K. A.; Beach, J. V.; Waymouth, R. M. *Polym. Prepr.* **1996**, *37*, (2), 297.

Acknowledgments

We wish to thank Paul Beeson of Sandia National Labs for performing photophysical measurements. We also thank Dr. Vincent Ortiz of Kansas State University for collaborative efforts in the *ab initio* modeling of oligosilanes and Dr. Robert Waymouth of Stanford University for helpful discussions and synthetic collaborations. This work was supported by the United States Department of Energy under Contract DE-AC04-

94AL85000. Sandia is a multiprogram laboratory operated by Sandia Corporation, a Lockheed Martin Company, for the United States Dpartment of Energy.

UNLIMITED RELEASE

INITIAL DISTRIBUTION

	Copies	
MS 0367	1	J. G. Curro
MS 1407	1	D. A. Loy
MS 9055	1	C. M. Rohlfing
MS 1405	1	G. M. Jamison
MS 9055	1	F. P. Tully
MS 1405	1	C. L. Renschler
MS 1407	1	J. H. Aubert
MS 1435	1	H. J. Saxton
MS 0188	1	LDRD Office
MS 0619	2	Review and Approval Desk, 12690 For DOE/OSTI
MS 0899	5	Technical Library, 4916
MS 9018	1	Central Technical Files, 8940-2